## COMMUNICATION

Check for updates

# Mechanism of poly(N-isopropylacrylamide) cononsolvency in aqueous methanol solutions explored *via* oxygen K-edge X-ray absorption spectroscopy†

Masanari Nagasaka, [ID] *[ab] Fumitoshi Kumaki, [ID] [c] Yifeng Yao, [ID] [d] Jun-ichi Adachi [ID] [ce] and Kenji Mochizuki [ID] [d]

The cononsolvency mechanism of poly(N-isopropylacrylamide) (PNIPAM), dissolving in pure methanol (MeOH) and water ($H_2O$) but being insoluble in MeOH–$H_2O$ mixtures, was investigated by O K-edge X-ray absorption spectroscopy (XAS). The cononsolvency emerges from the aggregation of PNIPAM with MeOH clusters, leading to the collapse of the hydrophobic hydration of PNIPAM.

## Introduction

PNIPAM is a stimuli-responsive polymer that is sensitive to various chemical environments, such as temperature and pH. This property translates to a low critical solution temperature, where it is dissolvable in solutions at low temperatures, known as a coil state, and is insoluble at high temperatures, known as a globule state.[1–3] PNIPAM is dissolved in pure MeOH and $H_2O$ at 25 °C but is insoluble in MeOH–$H_2O$ mixtures at the same temperature, which is known as cononsolvency.[4–6] The coil-to-globule-to-coil transition occurs at the same temperature, where PNIPAM stays in the coil state in pure $H_2O$, then transitions to the globule state by increasing the MeOH molar fraction, and transitions again to the coil state in pure MeOH.[7] This behaviour stems from the lower critical solution temperature in aqueous MeOH solution compared to that in pure MeOH and $H_2O$. Cononsolvency is a general phenomenon that emerges not only in polymers, but also in small molecules such as tertiary butyl alcohol in aqueous MeOH solutions.[8,9]

*a* Institute for Molecular Science, Myodaiji, Okazaki 444-8585, Japan.
  E-mail: nagasaka@ims.ac.jp
*b* Molecular Science Program, Graduate Institute for Advanced Studies, SOKENDAI,
  Myodaiji, Okazaki 444-8585, Japan
*c* Photon Factory, Institute of Materials Structure Science, High Energy Accelerator
  Research Organization, 1-1 Oho, Tsukuba, Ibaraki 305-0801, Japan
*d* Department of Chemistry, Zhejiang University, Hangzhou, 310028, P. R. China
*e* Materials Structure Science Program, Graduate Institute for Advanced Studies,
  SOKENDAI, 1-1 Oho, Tsukuba, Ibaraki 305-0801, Japan
† Electronic supplementary information (ESI) available. See DOI: https://doi.org/
  10.1039/d4cp00676c

Understanding the mechanism of polymer cononsolvency is paramount for comprehending the phase transition dynamics of biomolecules, including protein folding, DNA packing, and interchain complexation. Therefore, the mechanism of polymer cononsolvency has been investigated in several experimental and theoretical studies.[3,10,11] The cononsolvency of PNIPAM in aqueous MeOH solutions is driven by the competition between MeOH and $H_2O$ for the hydrogen bond (HB) of PNIPAM; conversely, PNIPAM dissolves in pure MeOH and $H_2O$ owing to the cooperative HB of solvent molecules.[12] The MeOH–$H_2O$ mixed cluster formation drives the cononsolvency of PNIPAM.[13,14] The polymer units aggregate owing to several factors, including the preferential binding of MeOH to PNIPAM,[15–17] geometric frustration due to the exchange of the molecular interaction of PNIPAM with $H_2O$ to that with MeOH,[18] an excluded volume effect from the methyl group of MeOH,[19] and the disruption of the HB structure of the NH group in PNIPAM with $H_2O$ owing to the existence of MeOH.[20] The coil-to-globule transition is related to the hydrophobic hydration of the isopropyl group in PNIPAM in the coil state and the collapse of hydration upon the addition of MeOH in the globule state.[21,22] However, the cononsolvency mechanism is still unknown because the molecular interactions of PNIPAM with MeOH and $H_2O$ have not been fully understood yet.

In this study, we investigated the molecular interactions of the C=O group in PNIPAM with MeOH and $H_2O$ from the energy shifts of the C=O $\pi^*$ peaks in the O K-edge XAS of PNIPAM along with molecular dynamics (MD) simulations and inner-shell calculations. XAS is advantageous for the element-selective structural analysis of light elements (C, N, O, *etc.*), as shown by its applicability to liquids and solutions.[23] However, XAS measurements in the transmission mode are difficult because soft X-rays are strongly absorbed by air and liquids. Recently, we performed *operando* XAS measurements of the chemical processes in solution by developing a transmission-type liquid cell, including a precise thickness control technique.[24,25] The C=O $\pi^*$ peak (532 eV) in PNIPAM can be observed *via* O K-edge XAS by separation of the contribution

from solvents MeOH and $H_2O$, whose first peaks are around 535 eV.[26,27]

## Results and discussion

Fig. 1 shows the O K-edge XAS spectra of PNIPAM in aqueous MeOH solutions $(MeOH)_x(H_2O)_{1-x}$ with different molar fractions at 25 °C. The XAS experiments were performed using a transmission-type liquid cell[24,25] at the soft X-ray beamline BL-7A of the Photon Factory, Institute of Materials Structure Science, High Energy Accelerator Research Organization (KEK-PF).[28] The C=O $\pi^*$ peaks of PNIPAM were observed at approximately 532 eV, and the strong absorbances of solvents MeOH and $H_2O$ were observed at the higher energy side. Note that soft X-rays above 535 eV cannot transmit the liquid layers because the thick liquid layers were prepared for the increase of the absorbance of the C=O $\pi^*$ peaks of PNIPAM. PNIPAM with 50 mg mL$^{-1}$ was dissolved in solutions considering the detection limit of C=O $\pi^*$ peaks in solvents MeOH and $H_2O$ (Section S1, ESI†). PNIPAM is insoluble at $0.4 > x > 0.1$ (Section S2, ESI†). The C=O $\pi^*$ peaks were not observed at $x = 0.4$ and $x = 0.2$ because the concentrations of PNIPAM are below the detection limit due to the formation of PNIPAM aggregates, whose details are discussed in Section S1 of the ESI.†

Fig. 2 shows the energy shift of the C=O $\pi^*$ peak in PNIPAM as a function of the MeOH molar fraction. The energetic positions of the C=O $\pi^*$ peaks were obtained by the fitting procedures shown in Fig. 1. We confirmed that the spectral fluctuations did not affect the energetic positions of the C=O $\pi^*$ peaks. The C=O $\pi^*$ peaks were not observed at $0.4 > x > 0.1$, denoting the cononsolvency region. The errors of the energetic positions were within 17 meV by the calibrations of the photon energies. By increasing the $H_2O$ molar fraction in the MeOH-rich region ($x > 0.4$), the C=O $\pi^*$ peaks exhibited higher energy shifts compared to that of pure MeOH ($x = 1.0$) as a slope of 51 meV/$(1 - x)$. The highest energy shift corresponding to the C=O $\pi^*$ peak at $x = 0.45$ was 27 meV. In contrast, in the $H_2O$-rich region ($0.1 > x$), notably higher energy shifts were recorded for the C=O $\pi^*$ peaks; specifically, the energy shift of the C=O $\pi^*$ peak in pure $H_2O$ ($x = 0.0$) was 127 meV. Although PNIPAM exhibits identical dissolution behaviours in MeOH and $H_2O$ at the macroscopic scale, the molecular interactions of PNIPAM with MeOH and $H_2O$ significantly differ at the microscopic scale, explaining the cononsolvency.

To reveal the origin of the energy shift of the C=O $\pi^*$ peak in PNIPAM, the structure of a single atactic 40-mer PNIPAM chain dissolved in 10 000 solvent molecules of MeOH and $H_2O$ was investigated by MD simulations using the GROMACS 2021.3 package.[29] The radius of gyration ($R_g$) was determined for different molar fractions of aqueous MeOH solutions to investigate the coil and globule states. The $R_g$ values at $x = 1.0$ (pure MeOH), $x = 0.2$, and $x = 0.0$ (pure $H_2O$) were calculated by averaging all the trajectories (Section S3, ESI†). Note that $x = 0.2$ was selected because it is near the middle region of cononsolvency ($0.4 > x > 0.1$). Table 1 lists the $R_g$ values at different molar fractions. At $x = 1.0$, $R_g = 1.99$, indicating that the PNIPAM chain spread in pure MeOH. Because $R_g = 1.78$ at $x = 0.0$, the polymer units of PNIPAM were inferred to remain close to each other in pure $H_2O$. The smallest $R_g$ value (= 1.71) was measured at $x = 0.2$, indicating that PNIPAM exhibited a globule state.

The coordination numbers of the HB structures of MeOH and $H_2O$ to the C=O group of PNIPAM were obtained by radial distribution function (RDF) analysis (Section S4, ESI†). As shown in Table 1, the coordination number of MeOH ($O_m$) to PNIPAM was 1.35 in pure MeOH ($x = 1.0$), indicating that one or two MeOH molecules were connected to the C=O group in PNIPAM. The two $H_2O$ molecules formed an HB structure with
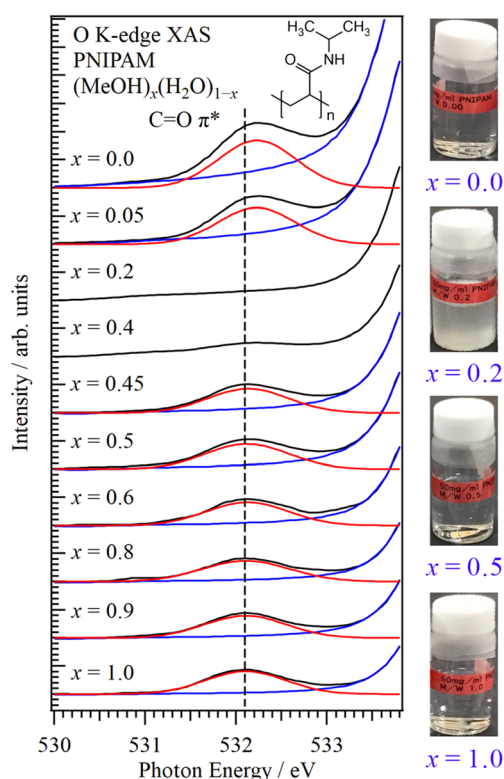


**Fig. 1** O K-edge XAS spectra of PNIPAM in aqueous MeOH solutions at different molar fractions. The energetic position of the C=O $\pi^*$ peak at $x = 1.0$ is indicated by the dashed line. The photos of PNIPAM in aqueous MeOH solutions are shown in the inset.
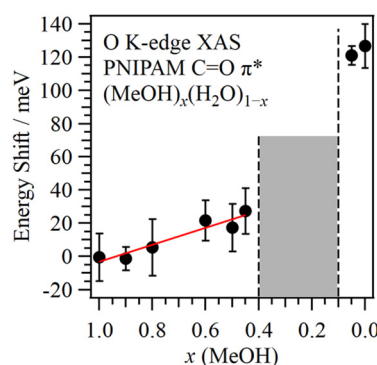


**Fig. 2** Energy shift of the C=O $\pi^*$ peak in PNIPAM as a function of MeOH molar fraction from pure MeOH ($x = 1.0$). The middle concentration region denotes cononsolvency.

This journal is © the Owner Societies 2024

*Phys. Chem. Chem. Phys.*, 2024, **26**, 13634–13638 | **13635**

**Table 1** Radii of gyration ($R_g$) of PNIPAM and average HB coordination numbers of $H_2O$ ($O_w$) and MeOH ($O_m$) with the C=O group of PNIPAM from MD simulations

|         | $R_g$/nm        | $O_w$           | $O_m$           |
| ------- | --------------- | --------------- | --------------- |
| $x = 0.0$ | $1.78 \pm 0.19$ | $2.10 \pm 0.03$ | —               |
| $x = 0.2$ | $1.71 \pm 0.17$ | $1.65 \pm 0.01$ | $0.34 \pm 0.01$ |
| $x = 1.0$ | $1.99 \pm 0.16$ | —               | $1.35 \pm 0.01$ |

PNIPAM in pure $H_2O$ ($x = 0.0$) because the coordination number of $H_2O$ ($O_w$) to PNIPAM was 2.10. Because $O_w = 1.65$ and $O_m = 0.34$ at $x = 0.2$, the $H_2O$ molecules could form HB structures with PNIPAM more easily compared to MeOH molecules. Approximately two solvent molecules were connected to the C=O group in PNIPAM at $x = 0.2$, owing to a total coordination number of 1.99. Upon increasing the molar fraction of $H_2O$ from pure MeOH, the HB structures with MeOH are substituted to those with $H_2O$. Specifically, the HB structures originally formed between PNIPAM and one or two MeOH molecules were replaced by interactions involving two $H_2O$ molecules.

Fig. 3 shows the O K-edge inner-shell spectra of the HB structures of PNIPAM and *N*-isopropylacrylamide (NIPAM), which is the polymer unit of PNIPAM, using the program package GSCF3.[30,31] The oxygen atom in the central polymer unit was considered only in the inner-shell calculations of PNIPAM. The structures of NIPAM and 5-mer PNIPAM chain were optimized including the solvent effect of MeOH using the polarizable continuum model (Section S5, ESI†). The HB model structures of NIPAM and PNIPAM were obtained from the distances and angles of the HB structures determined by two-



**Fig. 3** Calculated O K-edge inner-shell spectra of several HB structures of the C=O group in NIPAM or PNIPAM with $H_2O$ and MeOH molecules. The inset shows the HB structures of NIPAM or PNIPAM with $H_2O$ and MeOH molecules.

dimensional RDF analysis (Section S6, ESI†). Note that the inner-shell calculations of the HB model structures are qualitatively effective for discussing the relations of the energy shifts of the C=O $\pi^*$ peaks with the changes of the HB structures because the energy shifts reflect the intermolecular interactions.[25]

The C=O $\pi^*$ peaks in both NIPAM and PNIPAM showed higher energy shifts when the coordination numbers of the HB structures were increased and the HB structures involving MeOH were substituted with $H_2O$ (Section S7, ESI†). In the inner-shell spectra of NIPAM, the C=O $\pi^*$ peak in the HB structure of NIPAM with two $H_2O$ molecules showed a higher energy shift (43 meV) compared to that of MeOH + $H_2O$. The energy shift of the C=O $\pi^*$ peak in the HB structures of PNIPAM from MeOH + $H_2O$ to two $H_2O$ was 48 meV, approximating that of NIPAM. In contrast, in the same HB structures (MeOH + $H_2O$), the C=O $\pi^*$ peak in PNIPAM showed a tremendously higher energy shift (228 meV) than that in NIPAM. Note that the C=O $\pi^*$ peak in PNIPAM includes the interaction between the polymer units of PNIPAM owing to structural optimization, and that in NIPAM has no interaction of the polymer units, which resembles the chain structures of PNIPAM in liquid MeOH.

In the MeOH-rich region ($x > 0.4$), the C=O $\pi^*$ peak in the O K-edge XAS spectra showed a higher energy shift upon increasing the $H_2O$ molar fraction as a slope of 51 meV/($1 - x$). In the inner-shell calculations, the energy shift of the C=O $\pi^*$ peak in the HB structures of PNIPAM from MeOH + $H_2O$ to two $H_2O$ was 48 meV. Thus, the higher energy shift of the C=O $\pi^*$ peak in the MeOH-rich region indicated that the HB structure of the C=O group in PNIPAM with MeOH was substituted with its $H_2O$ equivalent by increasing the $H_2O$ molar fraction. The increase of the coordination number of MeOH and $H_2O$ also affected the higher energy shift of the C=O $\pi^*$ peak. These results were consistent with the MD simulations, in which the HB structures of PNIPAM with one or two MeOH molecules shifted to those with two $H_2O$ molecules by increasing the $H_2O$ molar fraction.

In the O K-edge XAS spectra, the C=O $\pi^*$ peak of PNIPAM in pure $H_2O$ ($x = 0.0$) showed a higher energy shift of 127 meV from that of pure MeOH ($x = 1.0$), which could not be explained by the simple substitution of the HB structures from MeOH to $H_2O$. In the inner-shell calculation, the energy shift of the C=O $\pi^*$ peak from NIPAM to PNIPAM was 228 meV in the same HB structures, indicating that the higher energy shift was induced by the increase of the interaction between polymer units. Because PNIPAM is dissolved in pure MeOH and $H_2O$, it was considered that the PNIPAM chains expanded in both MeOH and $H_2O$ solvents; however, this study proposes that PNIPAM forms rounded structures in pure $H_2O$, whereas it forms chain structures in pure MeOH. These results were consistent with the MD simulations, in which the $R_g$ value in pure $H_2O$ was inferior to that in pure MeOH.

Liquid MeOH forms one-dimensional chain structures.[32] The C=O group in PNIPAM formed HB structures with MeOH, and the isopropyl group in PNIPAM exhibited hydrophobic interactions with the methyl group in MeOH. Because liquid MeOH has a chain structure, the PNIPAM chains spread through the hydrophobic interactions of the MeOH chains. In
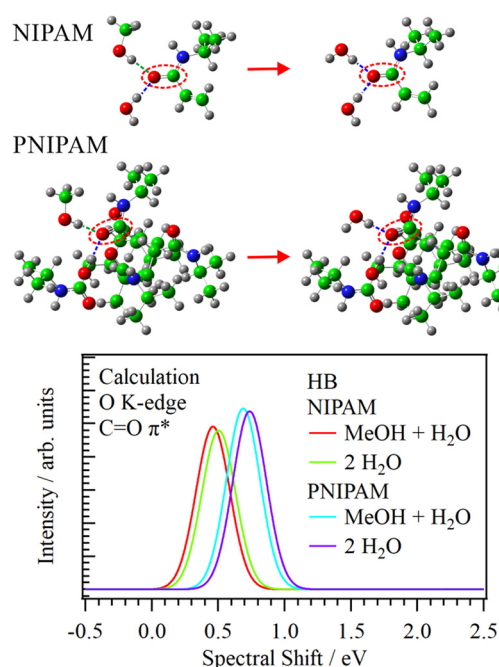
**13636** | *Phys. Chem. Chem. Phys.*, 2024, **26**, 13634–13638

This journal is © the Owner Societies 2024

contrast, $H_2O$ molecules formed a three-dimensional HB network and exhibited hydrophobic hydration of the isopropyl group in PNIPAM. PNIPAM shows rounded structures with the hydrophobic hydration of PNIPAM. Because the interaction between polymer units in pure $H_2O$ is larger than that in pure MeOH, the C=O $\pi^\star$ peak at pure $H_2O$ shows a higher energy shift (127 meV) compared to that in pure MeOH.

The structures of aqueous MeOH solutions were extensively investigated by several experimental and theoretical studies, which are summarized in Section S8 of the ESI.† We have also revealed from the C K-edge XAS of aqueous MeOH solutions that the hydrophobic clusters of MeOH are formed in the middle concentration region $(0.7 > x > 0.3)$.[27] Because MeOH shifts from chain structures to cluster ones by increasing the $H_2O$ molar fraction from pure MeOH, the polymer units of PNIPAM tend to gather by the hydrophobic interaction with MeOH clusters, leading to the deposition of PNIPAM at $x = 0.4$. This finding also supports that PNIPAM aggregates include 80% solvent MeOH and $H_2O$.[7] This was consistent with the smallest $R_g$ value $(x = 0.2)$ observed in the MD simulation. PNIPAM maintains a coil state in pure $H_2O$ $(x = 0.0)$ owing to the hydrophobic hydration of PNIPAM. By increasing the molar fraction of MeOH from pure $H_2O$, the hydrophobic hydration of PNIPAM was disrupted and the hydrophobic interaction of PNIPAM with MeOH increased,[21,22] inducing cononsolvency at $0.4 > x > 0.1$.

## Conclusions

The mechanism of PNIPAM cononsolvency in aqueous MeOH solutions was investigated from the molecular interactions of the C=O group in PNIPAM with MeOH and $H_2O$ using O K-edge XAS. The C=O $\pi^\star$ peak in pure $H_2O$ shows an extremely higher energy shift from pure MeOH, which cannot be explained by the simple substitution of the HB structure from MeOH to $H_2O$. The inner-shell calculation proposed that it is due to the increase of the interaction between polymer units, indicating PNIPAM in pure $H_2O$ is the rounded structure with the hydrophobic hydration of the isopropyl group in PNIPAM. Although PNIPAM is dissolved in pure MeOH and $H_2O$, this study proposes that PNIPAM forms rounded structures in pure $H_2O$, whereas it forms chain structures in pure MeOH. At $0.4 > x > 0.1$, the hydrophobic hydration of PNIPAM is interrupted by the addition of MeOH, whereas the hydrophobic interaction of PNIPAM with MeOH is enhanced. The polymer units of PNIPAM aggregated *via* the MeOH hydrophobic clusters, inducing cononsolvency. The concentration change of PNIPAM might lead to the different mechanism of cononsolvency, which would be the subject of future study.

The phase transition dynamics of polymers, such as cononsolvency and low critical solution temperature,[1–3] can be investigated using XAS from the molecular interactions of different groups in the polymers with solvent molecules. Thus, the element-selective analysis using XAS can be applied to the phase transition dynamics of biomolecules, such as protein folding, DNA packing, and interchain complexation.

## Author contributions

Masanari Nagasaka: conceptualization, data curation, formal analysis, funding acquisition, investigation, methodology, project administration, resources, supervision, validation, visualization, writing – original draft, writing – review & editing; Fumitoshi Kumaki: investigation, data curation, formal analysis, methodology; Yifeng Yao: investigation, data curation, formal analysis, methodology; Jun-ichi Adachi: investigation, methodology, validation; Kenji Mochizuki: investigation, data curation, formal analysis, funding acquisition, resources, validation, visualization, writing – original draft, writing – review & editing.

## Conflicts of interest

There are no conflicts to declare.

## Acknowledgements

## References

1 H. G. Schild, *Prog. Polym. Sci.*, 1992, **17**, 163–249.
2 E. S. Gil and S. M. Hudson, *Prog. Polym. Sci.*, 2004, **29**, 1173–1222.
3 A. Halperin, M. Kröger and F. M. Winnik, *Angew. Chem., Int. Ed.*, 2015, **54**, 15342–15367.
4 T. Amiya, Y. Hirokawa, Y. Hirose, Y. Li and T. Tanaka, *J. Chem. Phys.*, 1987, **86**, 2375–2379.
5 F. M. Winnik, H. Ringsdorf and J. Venzmer, *Macromolecules*, 1990, **23**, 2415–2416.
6 H. G. Schild, M. Muthukumar and D. A. Tirrell, *Macromolecules*, 1991, **24**, 948–952.
7 G. Zhang and C. Wu, *Phys. Rev. Lett.*, 2001, **86**, 822–825.
8 K. Mochizuki and K. Koga, *Phys. Chem. Chem. Phys.*, 2016, **18**, 16188–16195.
9 K. Mochizuki, S. R. Pattenaude and D. Ben-Amotz, *J. Am. Chem. Soc.*, 2016, **138**, 9045–9048.
10 C. Scherzinger, A. Schwarz, A. Bardow, K. Leonhard and W. Richtering, *Curr. Opin. Colloid Interface Sci.*, 2014, **19**, 84–94.
11 S. Bharadwaj, B.-J. Niebuur, K. Nothdurft, W. Richtering, N. F. A. van der Vegt and C. M. Papadakis, *Soft Matter*, 2022, **18**, 2884–2909.
12 F. Tanaka, T. Koga and F. M. Winnik, *Phys. Rev. Lett.*, 2008, **101**, 028302.

This journal is © the Owner Societies 2024

*Phys. Chem. Chem. Phys.*, 2024, **26**, 13634–13638 | **13637**

13 G. Zhang and C. Wu, *J. Am. Chem. Soc.*, 2001, **123**, 1376–1380.

14 J. Pang, H. Yang, J. Ma and R. Cheng, *J. Phys. Chem. B*, 2010, **114**, 8652–8658.

15 J. Walter, J. Sehrt, J. Vrabec and H. Hasse, *J. Phys. Chem. B*, 2012, **116**, 5251–5259.

16 D. Mukherji, C. M. Marques and K. Kremer, *Nat. Commun.*, 2014, **5**, 4882.

17 F. Rodríguez-Ropero, T. Hajari and N. F. A. van der Vegt, *J. Phys. Chem. B*, 2015, **119**, 15780–15788.

18 A. Pica and G. Graziano, *Phys. Chem. Chem. Phys.*, 2016, **18**, 25601–25608.

19 K. Mochizuki, *J. Phys. Chem. B*, 2020, **124**, 9951–9957.

20 C. Dalgicdir, F. Rodríguez-Ropero and N. F. A. van der Vegt, *J. Phys. Chem. B*, 2017, **121**, 7741–7748.

21 I. Bischofberger, D. C. E. Calzolari, P. De Los Rios, I. Jelezarov and V. Trappe, *Sci. Rep.*, 2014, **4**, 4377.

22 K. Kyriakos, M. Philipp, C.-H. Lin, M. Dyakonova, N. Vishnevetskaya, I. Grillo, A. Zaccone, A. Miasnikova, A. Laschewsky, P. Müller-Buschbaum and C. M. Papadakis, *Macromol. Rapid Commun.*, 2016, **37**, 420–425.

23 J. W. Smith and R. J. Saykally, *Chem. Rev.*, 2017, **117**, 13909–13934.

24 M. Nagasaka, H. Yuzawa and N. Kosugi, *Anal. Sci.*, 2020, **36**, 95–105.

25 M. Nagasaka and N. Kosugi, *Chem. Lett.*, 2021, **50**, 956–964.

26 T. Tokushima, Y. Horikawa, Y. Harada, O. Takahashi, A. Hiraya and S. Shin, *Phys. Chem. Chem. Phys.*, 2009, **11**, 1679–1682.

27 M. Nagasaka, K. Mochizuki, V. Leloup and N. Kosugi, *J. Phys. Chem. B*, 2014, **118**, 4388–4396.

28 K. Amemiya, H. Kondoh, T. Yokoyama and T. Ohta, *J. Electron Spectrosc. Relat. Phenom.*, 2002, **124**, 151–164.

29 M. J. Abraham, T. Murtola, R. Schulz, S. Páll, J. C. Smith, B. Hess and E. Lindahl, *SoftwareX*, 2015, **1–2**, 19–25.

30 N. Kosugi and H. Kuroda, *Chem. Phys. Lett.*, 1980, **74**, 490–493.

31 N. Kosugi, *Theor. Chim. Acta*, 1987, **72**, 149–173.

32 T. Yamaguchi, K. Hidaka and A. K. Soper, *Mol. Phys.*, 1999, **96**, 1159–1168.